Appl Phys A (2012) 109:81–85
DOI 10.1007/s00339-012-7051-y

Applied Physics A
Materials Science & Processing

Graphene oxide as a substrate for Raman enhancement

Weizi Liang · Xiaoyun Chen · Yu Sa · Yuanming Feng · Yan Wang · Wang Lin

Received: 30 June 2012 / Accepted: 3 July 2012 / Published online: 18 July 2012

Abstract We report the properties of graphene oxide, a two-dimensional carbon nanomaterial, as a substrate for surface-enhanced Raman scattering. The graphene oxide substrate produced Raman enhancement for rhodamine 6G, melamine, and cephalexin. Intense characteristic D and G peaks of graphene oxide were observed when positively charged rhodamine 6G and melamine were used as the Raman probe. We attribute the appearance of D and G peaks to the aggregation of negatively charged graphene oxide.

1 Introduction

Graphene, a single atomic planar sheet of sp^2 bonded carbon atoms, shows extreme physical properties arising from the two-dimensional hexagonal lattice structure [1, 2]. Many unusual properties have been discovered in grapheme, including the linear low energy electronic dispersion [1], unconventional quantum Hall effect [2], ballistic transport [3], superior thermal conductivity [4, 5], and high mechanical strength [6]. These unique properties make graphene a promising candidate for future electronic devices [7–9]. Of our particular interest, the application of graphene provides a new sight to investigate the mechanism of surface-enhanced Raman spectroscopy (SERS). Surface-enhanced Raman scattering originates from molecules that are in the vicinity of small metal particles or rough surfaces of conductive material, particularly silver and gold [10, 11]. Although surface-enhanced Raman spectroscopy has been widely used to study molecules with low concentrations [12], the exact mechanism of SERS is still under debate [13, 14]. It is generally accepted that the enhancement of Raman scattering is from an electromagnetic mechanism and a chemical (charge-transfer) mechanism. Electromagnetic mechanism is based on the local electromagnetic enhancement, while chemical mechanism is based on the charge transfer between the molecules and the substrate [14, 15]. The two mechanisms are usually entangled to generate enhanced Raman signals. Ling [16] proposed that graphene or graphene oxide can be used as the SERS substrate to study the charge-transfer mechanism of Raman enhancement. Jung [17] observed the strong Raman scattering from iodine anions adsorbed on single layer graphene, attributing the large Raman signal to intramolecular electronic resonance enhancement.

Similar to graphene, graphene oxide (GO) is a non-stoichiometric two-dimensional carbon sheet prepared in bulk quantities through oxidative exfoliation of graphite [18–20]. Graphene oxide contains hydroxyl and epoxy functional groups on either side of its basal plane, while carboxyl groups are located at the edge sites [21, 22]. The oxygen functional groups make the GO surface a reactive site for ionic and nonionic interactions by binding molecules [23–26]. Therefore, GO can be considered as a weak cation exchanger due to its ionizable carboxyl groups, which exchange cation with positively charged organic molecules. As for surface-enhanced Raman scattering, the versatile GO/molecules bindings would be intriguing and suitable to study the Raman enhancement mechanism [27, 28]. Motivated by the ionization properties of functionalized GO, we investigated herein the properties of GO as a substrate for surface-enhanced Raman scattering, where a distinction from different ionized molecules can be observed.

W. Liang · X. Chen · Y. Sa · Y. Feng · Y. Wang · W. Lin (✉)
Department of Biomedical Engineering,
College of Precision Instrument and Optoelectronics Engineering,
Tianjin University, Tianjin 300072, China
e-mail: wlin@tju.edu.cn
Fax: +86-22-27892060

2 Experimental

GO was prepared according to a modified Hummers method [29, 30]. The GO powder was dispersed in water for various wt/wt% (weight by weight percent) concentrations by sonication. Then, the GO solution was deposited on the SiO_2/Si system and dried in air. To test the Raman enhancement, the probing molecules were dripped onto the GO substrates and followed by drying in air. The Raman signals of probing molecules were detected using a Raman microscope spectroscopy (Renishaw inVia) with a laser wavelength of 532 nm. Electron images were recorded with use of a JEM-100 CXII Transmission Electron Microscope from JEOL, with a 100 kV acceleration tension.

3 Results and discussion

Figure 1 shows TEM image of 10^{-3} mg/mL GO sheets deposited on the SiO_2/Si surface. Inspection of the TEM image indicates that the GO sheets are uniformly distributed on the SiO_2/Si surface. There is no evidence for aggregation or phase separation of the GO sheets. The presence of GO in the samples was confirmed by the Raman spectra, as shown in Fig. 2. The Raman spectra have been used extensively in the characterization of graphene and carbon nanostructures. GO dispersion solutions of various concentrations were deposited on SiO_2/Si system and characterized by Raman spectra. The two most typical features in the 600–1800 cm^{-1} region are the G and D peaks, which lie at around 1595 and 1352 cm^{-1}, respectively. The G peak is due to the doubly degenerate zone center E2g mode. From molecular point of view, the D peak is due to the breathing modes of sp^2 atoms in defected graphite [31], while, from solid-state point of view, the D peak may arise as resonant Raman coupling [32] or double resonance mechanism [33, 34]. The peak centered at 960 cm^{-1} corresponds to two-phonon transverse optical modes of Si [16].

To test the Raman enhancement, three molecules, rhodamine 6G (R6G), melamine, and cephalexin, are used as the probe, shown as Scheme 1. The three molecules have different ionization states, leading to different binding strength with negative charged GO sheet [35]. It has been reported that the ionic strength plays an important role in the behavior of R6G molecules in water [36]. The soluble dye molecules of R6G ionized in water, and the positively charged $(R6G)^+$ ions move towards the negatively charged GO [37]. Melamine molecule shows the positive ion characteristics, which is assigned to the composition $C_3H_7N_6^+$ and corresponds to $(melamine + H)^+$ [38]. In addition, melamine is considered to be a suitable molecular precursor compound for polymerized forms of carbon nitride, which may cross-link GO by the three amino groups ($–NH_2$) on melamine molecules [39]. Cephalexin molecules contain both the amino group and the carboxyl group, making the ionization state of cephalexin molecules varied with pH in aqueous solutions. Cephalexin molecules are negatively charged for pH above 5.88 and keep electrically neutral for pH between 2.56 and 5.88 [40], resulting in a weak binding with GO sheet, if any.

Figure 3 shows the Raman spectra of 10^{-5} M R6G on GO substrates prepared from various GO dispersion solutions. The Raman peaks at 614 (C–C–C ring), 775 (C–H bending), 1185, 1312, 1363 (aromatic C–C stretching), 1505 (aromatic C–C stretching), 1572 (aromatic C–C stretching), and 1650 cm^{-1} (aromatic C–C stretching) are characteristic vibration of R6G molecules [41, 42]. In this experiment, 10^{-1}, 10^{-2}, and 10^{-3} mg/mL GO dispersion solutions were deposited on SiO_2/Si system to fabricate SERS substrates. At higher concentrations of GO substrates, relatively more intense Raman signals are observed compared to the lower concentrated GO substrates. However, strong D and G peaks are shown for the higher concentrated GO substrates. An extreme case is that, for the highest concentrated GO substrate, R6G peaks are overwhelmed by D and G peaks of GO. This

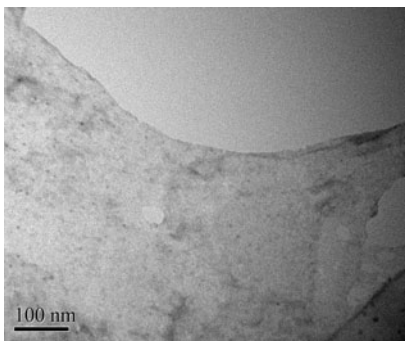

Fig. 1 TEM image of 10^{-3} mg/mL GO sheets deposited on a SiO_2/Si surface

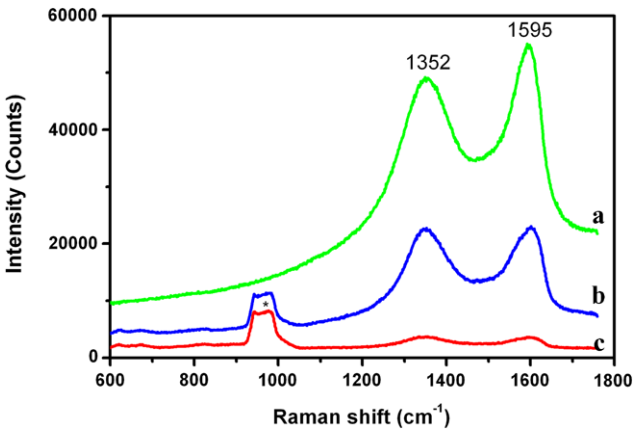

Fig. 2 Raman spectra of GO substrates prepared from (**a**) 10^{-1} mg/mL, (**b**) 10^{-3} mg/mL, and (**c**) 10^{-4} mg/mL GO dispersion solutions. The peak centered at 960 cm^{-1} (marked as *) corresponds to two-phonon transverse optical modes of Si

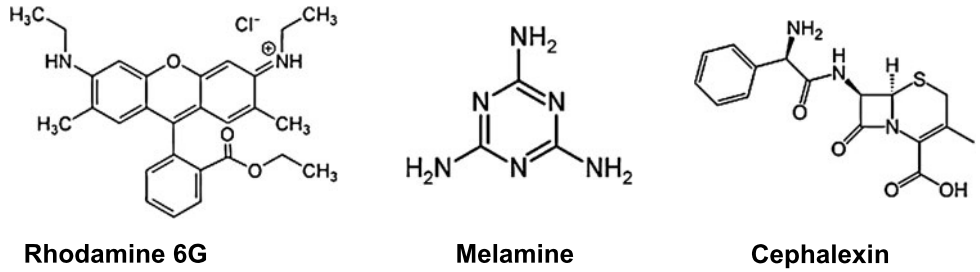

Scheme 1 The molecular structure of rhodamine 6G, melamine, and cephalexin

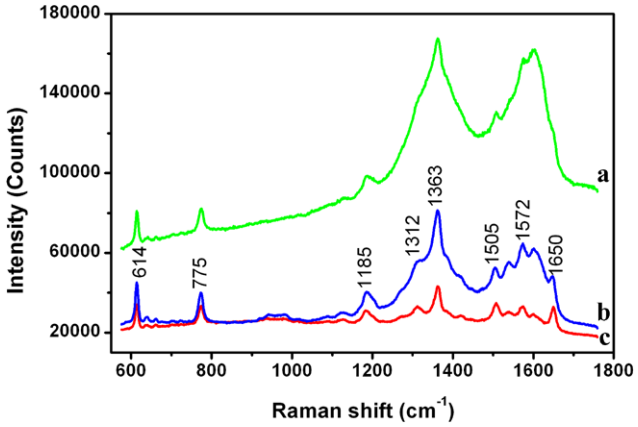

Fig. 3 Raman spectra of 10^{-5} M R6G on GO substrates prepared from (**a**) 10^{-1} mg/mL, (**b**) 10^{-2} mg/mL, and (**c**) 10^{-3} mg/mL GO dispersion solutions

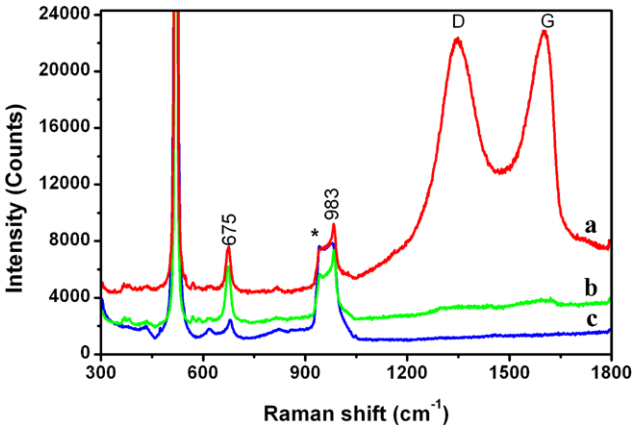

Fig. 4 Raman spectra of 10^{-4} M melamine on (**c**) SiO_2/Si substrate and GO substrates prepared from (**a**) 10^{-3} mg/mL and (**b**) 10^{-4} mg/mL GO dispersion solutions. The peak centered at 960 cm^{-1} (marked as *) corresponds to two-phonon transverse optical modes of Si

result indicates GO substrates may have some Raman enhancement functions, while D and G peaks become stronger for increasing concentrated GO substrates.

The graphene oxide is negatively charged due to residual defects such as carboxyl, hydroxyl, and epoxy groups [35]. Among the probing molecules we checked for Raman enhancement, R6G and melamine are positively charged molecules [37, 38]. Figure 4 shows the Raman spectra of 10^{-4} M melamine on SiO_2/Si substrate and GO substrates. The GO substrates were fabricated by depositing 10^{-3} or 10^{-4} mg/mL GO dispersion solutions onto the SiO_2/Si system. The Raman spectra show characteristic vibration peaks of melamine molecule at 675 and 983 cm^{-1}, denoting an in-plane deformation vibration mode and a ring breathing vibration mode, respectively [43], whereas those centered at 960 cm^{-1} correspond to two-phonon transverse optical modes of Si [16]. Notably, relatively more intense Raman signals of melamine molecules can be observed at higher concentrations of GO substrates, compared to that at lower concentrated GO substrates. Upon increasing GO concentration to 10^{-3} mg/mL, D and G peaks of GO molecules become intense. The result is quite similar to what we observed for R6G molecules. In Fig. 4, GO is less concentrated to observe D and G peaks than that used for R6G molecules. This may be because R6G is a strong Raman probing molecule. A higher concentrated GO substrate is needed to show D and G peaks from the strong Raman signals of R6G. Another possible reason is that melamine may polymerize GO sheets, because melamine molecules may cross-link GO by the three amino groups ($–NH_2$) on melamine [39].

Although it is straightforward to observe the characteristic peaks of GO with increasing GO concentrations, negatively charged probing molecules may show different behavior (Fig. 5). Cephalexin is a negatively charged molecule in water, leading to a weak binding with negatively charged GO sheets. Most notably, a Raman enhancement can be observed with increasing GO concentrations. The characteristic Raman peaks may be assigned as follows: 618 (aromatic ring bending), 755 (ring breathing), 1188 (aromatic C–H bending), 1359 (C–O stretching), 1603, and 1646 cm^{-1} (aromatic C–C stretching), whereas those centered at 960 cm^{-1} correspond to two-phonon transverse optical modes of Si [16]. It is worth noting that no discernible D and G peaks appear in Fig. 5, in contrast to intense D and G peaks of GO in R6G and melamine experiments. A possible mechanism is that negatively charged GO may aggregate to the positively charged R6G and melamine molecules. The aggregation of GO sheets leads to intense G and D peaks,

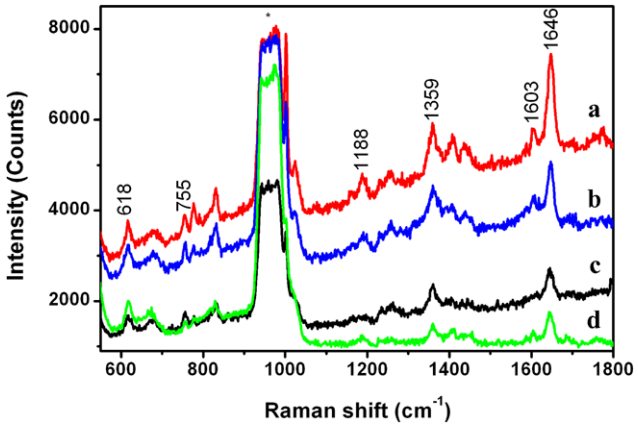

Fig. 5 Raman spectra of 10^{-3} M cephalexin on (**d**) SiO_2/Si substrate and GO substrates prepared from (**a**) 10^{-2} mg/mL, (**b**) 10^{-3} mg/mL, and (**c**) 10^{-4} mg/mL GO dispersion solutions. The peak centered at 960 cm^{-1} (marked as *) corresponds to two-phonon transverse optical modes of Si

shown in Figs. 3 and 4. The mechanism is reasonable in that the Raman spectra of negatively charged cephalexin show an opposite behavior. Recently, a similar phenomenon has been observed when Au nanoparticles capped with electrically neutral [44] 2-mercaptopyridine was attached to the GO sheets [45]. The characteristic peaks of 2-mercaptopyridine disappeared and only D and G peaks of GO remained.

It is widely accepted that the enhancement of Raman scattering is from two competing mechanisms, i.e., the electromagnetic mechanism and the chemical (charge transfer) mechanism. The results in this work appear to be more reasonably explained through the chemical mechanism, with a weak enhancement due to charge-transfer processes via the cluster active sites [14, 15].

4 Conclusions

A Raman enhancement substrate based on graphene oxide has produced Raman enhanced spectra for R6G, melamine, and cephalexin. The intense characteristic peaks of graphene oxide are captured in Raman spectra, which relates to the ionization state of probing molecules. The application of graphene oxide as the substrate may provide a new sight to study the mechanism of surface-enhanced Raman scattering.

Acknowledgements The authors acknowledge funding from the National Natural Science Foundation of China (NSFC) No. 31000784 and 81171342.

References

1. A.K. Geim, K.S. Novoselov, Nat. Mater. **6**, 183 (2007)
2. K.S. Novoselov, A.K. Geim, S.V. Morozov, D. Jiang, Y. Zhang, S.V. Dubonos, I.V. Grigorieva, A.A. Firsov, Science **306**, 666 (2004)
3. K.S. Novoselov, A.K. Geim, S.V. Morozov, D. Jiang, M.I. Katsnelson, I.V. Grigorieva, S.V. Dubonos, A.A. Firsov, Nature **438**, 197 (2005)
4. A.A. Balandin, S. Ghosh, W. Bao, I. Calizo, D. Teweldebrhan, F. Miao, C.N. Lau, Nano Lett. **8**, 902 (2008)
5. J.H. Seol, I. Jo, A.L. Moore, L. Lindsay, Z.H. Aitken, M.T. Pettes, X. Li, Z. Yao, R. Huang, D. Broido, N. Mingo, R.S. Ruoff, L. Shi, Science **328**, 213 (2010)
6. C. Lee, X. Wei, J.W. Kysar, J. Hone, Science **321**, 385 (2008)
7. X.L. Li, G.Y. Zhang, X.D. Bai, X.M. Sun, X.R. Wang, E. Wang, H.J. Dai, Nat. Nanotechnol. **3**, 538 (2008)
8. M.D. Stoller, S.J. Park, Y.W. Zhu, J.H. An, R.S. Ruoff, Nano Lett. **8**, 3498 (2008)
9. Y. Wang, Z.Q. Shi, Y. Huang, Y.F. Ma, C.Y. Wang, M.M. Chen, Y.S. Chen, Phys. Chem. C **113**, 13103 (2009)
10. J.R. Lombardi, R.L. Birke, Acc. Chem. Res. **42**, 734 (2009)
11. M. Fleischmann, P.J. Hendra, A.J. Mcquilla, Chem. Phys. Lett. **26**, 163 (1974)
12. K. Kneipp, H. Kneipp, I. Itzkan, R.R. Dasari, M.S. Feld, Chem. Rev. **99**, 2957 (1999)
13. L. Jensen, C.M. Aikens, G.C. Schatz, Chem. Soc. Rev. **37**, 1061 (2008)
14. B.N.J. Persson, K. Zhao, Z.Y. Zhang, Phys. Rev. Lett. **96**, 207401 (2006)
15. A. Otto, I. Mrozek, H. Grabhorn, W.J. Akemann, Phys. Condens. Matter **4**, 1143 (1992)
16. X. Ling, L. Xie, Y. Fang, H. Xu, H. Zhang, J. Kong, M.S. Dresselhaus, J. Zhang, Z. Liu, Nano Lett. **10**, 553 (2010)
17. N. Jung, A.C. Crowther, N. Kim, P. Kim, L. Brus, ACS Nano **4**, 7005 (2010)
18. W.S. Hummers, R.E. Offeman, J. Am. Chem. Soc. **80**, 1339 (1958)
19. N.I. Kovtyukhova, P.J. Ollivier, B.R. Martin, T.E. Mallouk, S.A. Chizhik, E.V. Buzaneva, A.D. Gorchinskiy, Chem. Mater. **11**, 771 (1999)
20. Y. Xu, H. Bai, G. Lu, C. Li, G. Shi, J. Am. Chem. Soc. **130**, 5856 (2008)
21. A. Lerf, H. He, M. Forster, J. Klinowski, J. Phys. Chem. B **102**, 4477 (1998)
22. D.A. Dikin, S. Stankovich, E.J. Zimney, R.D. Piner, G.H.B. Dommett, G. Evmenenko, S.T. Nguyen, R.S. Ruoff, Nature **448**, 457 (2007)
23. Y.J. Guo, S.J. Guo, J.T. Ren, Y.M. Zhai, S.J. Dong, E.K. Wang, ACS Nano **4**, 4001 (2010)
24. J. Balapanuru, J.X. Yang, S. Xiao, Q. Bao, M. Jahan, L. Polavarapu, J. Wei, Q.H. Xu, K.P. Loh, Angew. Chem., Int. Ed. Engl. **49**, 6549 (2010)
25. L.F. Wang, F.H. Yang, R.T. Yang, M.A. Miller, Ind. Eng. Chem. Res. **48**, 2920 (2009)
26. G. Goncalves, P.A.A.P. Marques, C.M. Granadeiro, H.I.S. Nogueira, M.K. Singh, J. Gracio, Chem. Mater. **21**, 4796 (2009)
27. X. Liu, L. Cao, W. Song, K. Ai, L. Lu, ACS Appl. Mater. Interfaces **3**, 2944 (2011)
28. X. Yu, H. Cai, W. Zhang, X. Li, N. Pan, Y. Luo, X. Wang, J.G. Hou, ACS Nano **5**, 952 (2011)
29. H.A. Becerril, J. Mao, Z. Liu, R.M. Stoltenberg, Z. Bao, Y. Chen, ACS Nano **2**, 463 (2008)
30. M. Hirata, T. Gotou, S. Horiuchi, M. Fujiwara, M. Ohba, Carbon **42**, 2929 (2004)
31. F. Tuinstra, J. Koenig, J. Chem. Phys. **53**, 1126 (1970)
32. I. Pocsik, M. Hundhausen, M. Koos, L. Ley, J. Non-Cryst. Solids **227–230**, 1083 (1998)
33. C. Thomsen, S. Reich, Phys. Rev. Lett. **85**, 5214 (2000)
34. A.V. Baranov, A.N. Bekhterev, Y.S. Bobovich, V.I. Petrov, Opt. Spektrosk. **62**, 1036 (1987)
35. V.C. Tung, M.J. Allen, Y. Yang, R.B. Kaner, Nat. Nanotechnol. **4**, 25 (2009)

36. X.Y. Zheng, A. Harata, T. Ogawa, Spectrochim. Acta, Part A, Mol. Biomol. Spectrosc. **57**, 315 (2001)
37. J. Taguchi, T. Yano, S. Habuchi, M. Vacha, S. Shibata, Thin Solid Films **519**, 6106 (2011)
38. G. Coullerez, D. Léonard, S. Lundmark, H.J. Mathieu, Surf. Interface Anal. **29**, 431 (2000)
39. B. Jürgens, E. Irran, J. Senker, P. Kroll, H. Müller, W. Schnick, J. Am. Chem. Soc. **125**, 10288 (2003)
40. K.Y. Wang, T. Chung, J. Membr. Sci. **247**, 37 (2005)
41. P. Hildebrandt, M. Stockburger, J. Phys. Chem. **88**, 5935 (1984)
42. A.M. Michaels, J. Jiang, L. Brus, J. Phys. Chem. B **104**, 11965 (2000)
43. Y. Cheng, Y. Dong, J. Wu, X. Yang, H. Bai, H. Zheng, D. Ren, Y. Zou, M. Li, J. Food Compos. Anal. **23**, 199 (2010)
44. Y.S. Pang, H.J. Hwang, M.S. Kim, J. Mol. Struct. **441**, 63 (1998)
45. J. Huang, L. Zhang, B. Chen, N. Ji, F. Chen, Y. Zhang, Z. Zhang, Nanoscale **2**, 2733 (2010)